

1

Supporting Information

2 **In-depth evaluation of automated non-contact reflectance-based hematocrit prediction of**
3 **dried blood spots**

4 Laura Boffel^{1#}, Liesl Heughebaert^{1#}, Stijn Lambrecht², Marc Luginbühl³ and Christophe P. Stove^{1*}

5 ¹Laboratory of Toxicology, Department of Bioanalysis, Faculty of Pharmaceutical Sciences, B-9000
6 Ghent

7 ²Laboratory of Clinical Chemistry and Hematology, Ghent University Hospital, B-9000 Ghent

8 ³CAMAG, Sonnenmattstrasse 11, CH-4132 Muttenz

9 #Equally contributed as co-first authors

10 *Corresponding author: Ottergemsesteenweg 460, B-9000 Ghent

11 christophe.stove@ugent.be

12

13 Supplementary Information Content

14	1.	Experimental section	2
15	1.1	Selection of measurement conditions	2
16	2.	Results and discussion	4
17	2.1	Selection of measurement conditions	4
18	3.	References	6
19	4.	Supplementary Tables	7
20	5.	Supplementary Figures	10

21

22

23 1. Experimental section

24 1.1 Selection of measurement conditions

25 The CAMAG® DBS-MS 500 HCT allows to adjust different instrumental parameters to determine the
26 hematocrit (Hct) of a dried blood spot (DBS). Therefore, prior to the set-up of the calibration model,
27 two instrumental parameters were optimized: (i) probe-to-card distance and (ii) integration time of
28 one measurement. The number of ‘sub-scans’ per individual measurement was fixed and set at 16, as
29 recommended by Luginbühl *et al.*¹

30 Optimization was performed using 24 venous left-over patient samples (Hct range 0.177 to 0.562 L/L).
31 In a first step, the probe-to-card distance was varied from 3 to 12 mm, increasing with 1 mm per
32 measurement and using a fixed integration time of 4500 μs. Also a probe-to-card distance of 6.4 mm
33 with a fixed integration time of 4500 μs was evaluated, as these were the initial instrumental settings
34 entered in the Chronos for CAMAG software. When oversaturation of the detector at a certain probe-
35 to-card distance was observed (i.e. a background (BG) reflectance > 840), the integration time was
36 reduced until the BG reflectance was below 840. Next, the optimal combination of probe-to-card
37 distance and integration time was chosen based on the back-calculated Hct of the samples, using an
38 initial linear calibration model. Based on the performance of the manual Hct prediction procedures²⁻⁴,
39 the acceptance limit was set at ±0.050 L/L difference from the reference value (determined using a
40 hematology analyzer).

41 In addition to the aforementioned measurement conditions, the use of multiple measurements
42 (further referred to as ‘scans’, with one ‘scan’ being the average of 16 ‘sub-scans’) per DBS to
43 determine the Hct was evaluated. First, as the reflectance of the DBS can be measured at different
44 positions within the spot, the maximum x- and y-position of the probe to the center of the DBS where
45 no BG reflectance is measured, was determined based on the mean diameter of a 25 μL DBS (n = 24;
46 Hct range 0.177 to 0.562 L/L). In a next step, to evaluate the ideal number of ‘scans’ per DBS (n), a
47 sample with a low (0.177 L/L), median (0.406 L/L) and high (0.562 L/L) Hct were ‘scanned’ at 21
48 different positions (Fig. S-11). For each sample, n was calculated using equation 1, in order to achieve
49 a relative uncertainty of the mean normalized reflectance (i.e. $BG_{\text{reflectance}}/Hct_{\text{reflectance}}$) of maximum 5%.

$$50 \quad \frac{CI_{(\alpha, n-1)}}{\text{mean}} \leq 0.05 \text{ with } CI_{(\alpha, n-1)} = t_{(\alpha, n-1)} \cdot \frac{SD}{\sqrt{n}} \pm \text{mean} \quad (1)$$

51 The mean and standard deviation (SD) were calculated based on the data obtained from 21 ‘scans’ and
52 a two-tailed t-distribution and $\alpha = 0.05$ were considered. The final number of ‘scans’ per DBS used in
53 all further experiments was based on the mean of the result obtained for the three samples.

54 Finally, multiple scans at the center vs. determination of the Hct at different positions within the spot
55 ('grid') were compared based on the data obtained during the set-up and validation of the calibration
56 model.

57 2. Results and discussion

58 2.1 Selection of measurement conditions

59 When the probe-to-card distance was varied from 3 to 12 mm at a fixed integration time of 4500 μ s,
60 oversaturation of the detector was observed for a probe-to-card distance of 3, 4 and 5 mm. Therefore,
61 the integration time was decreased to 1500, 2000 and 3000 μ s, respectively (Table S-6). Furthermore,
62 a probe-to-card distance of 6.4 mm in combination with an integration time of 4500 μ s yielded the
63 highest number of samples (92%) for which the back-calculated Hct values were within 0.050 L/L of
64 the reference value (Table S-7). Hence, 6.4 mm and 4500 μ s were selected as the optimal measurement
65 conditions, which were in fact the initial instrumental parameters entered in the Chronos for CAMAG
66 software. Since a non-weighted, linear regression equation to calculate the Hct was described in the
67 CAMAG DBS-MS 500 HCT manual, Hct values were back-calculated based on an initial, non-validated
68 linear calibration model.⁵ In addition, a linear calibration model was used by Luginbühl *et al.* to predict
69 the Hct of DBS in the context of a pharmacokinetic study of diclofenac.¹ Also here, the probe-to-card
70 distance was evaluated, by varying the distance from 0.5 to 2.5 mm.¹ The authors concluded that the
71 optimal probe-to-card distance was actually a range from 1.4 to 2.0 mm and continued with a distance
72 of 1.8 mm for further experiments. However, we could not reproduce the recommended standard
73 probe-to-card distance of 1.8 mm since the initial measurements were done using a vertical-positioned
74 probe (prototype, Fig. S-12). Our system on the other hand, has a tilted probe with a minimal probe-
75 to-card distance of 3 mm. More recently, Luginbühl *et al.* described the application of the automated
76 Hct prediction method to correct for a Hct-dependent bias for the analysis of phosphatidylethanol,
77 where a probe-to-card distance of 1.4 mm was applied to determine the Hct of the samples. Although
78 this distance is within the previously validated range, it is inconsistent with the probe-to-card distance
79 of 1.8 mm previously applied by these authors.^{1, 6} Therefore, re-evaluation of the optimal probe-to-
80 card distance was needed. Furthermore, since only a probe-to-card distance in a very low range (from
81 0.5 to 2.5 mm) was evaluated in these articles, back-calculated Hct values were only evaluated using a
82 probe-to-card distance up till 7 mm. Additionally, when using a probe-to-card distance of 8 mm and
83 higher, the beam of the excitation light appeared to be less focused on the DBS, with a less dense
84 coverage of the DBS at the outer edge of the light beam, compared to when using a probe distance of
85 7 mm and lower (Fig. S-13).

86 The 'ideal' number of 'scans' per DBS for a sample with a low (0.177 L/L), median (0.406 L/L) and high
87 (0.562 L/L) Hct were 5.9, 4.8 and 4.5, respectively, with a mean of 5 'scans' per DBS. Therefore, in all
88 further experiments all samples were measured in fivefold either at the center of the DBS or using a
89 grid. In addition, the mean diameter of a 25 μ L DBS was approximately 8 mm, while the diameter of

90 the area of the light beam covering the DBS was approximately 4 mm. Consequently, to avoid
91 measurement of the BG when analyzing smaller DBS, the maximum x- and y-position of the probe from
92 the center of the spot used in the grid was set at 1.5 mm (Fig. S-4).

93 3. References

- 94 1. M. Luginbühl, Y. Fischer and S. Gaugler, *Journal of analytical toxicology*, 2020, **46**, 187-193.
95 2. S. Capiou, L. S. Wilk, M. C. Aalders and C. P. Stove, *Analytical chemistry*, 2016, **88**, 6538-6546.
96 3. S. Capiou, L. S. Wilk, P. M. M. De Kesel, M. C. G. Aalders and C. P. Stove, *Analytical chemistry*,
97 2018, **90**, 1795-1804.
98 4. L. Delahaye, L. Heughebaert, C. Luhr, S. Lambrecht and C. P. Stove, *Clinica chimica acta;*
99 *international journal of clinical chemistry*, 2021, **523**, 239-246.
100 5. CAMAG, DBS-MS 500 HCT., [https://dbs.camag.com/product/camag-dbs-ms-500-](https://dbs.camag.com/product/camag-dbs-ms-500-hct#downloads)
101 [hct#downloads](https://dbs.camag.com/product/camag-dbs-ms-500-hct#downloads), (accessed 08/07/2022).
102 6. M. Luginbühl, F. Stoth, W. Weinmann and S. Gaugler, *Alcohol (Fayetteville, N.Y.)*, 2021, **94**, 17-
103 23.

104

105 4. Supplementary Tables

106 Table S-1. Number of calibrators and QC samples (n) allocated to the different Hct cohorts: < 0.20,
 107 0.20-0.25, 0.25-0.30, 0.30-0.35, 0.35-0.40, 0.40-0.45, 0.45-0.50 and > 0.50.

Hct cohort	< 0.20	0.20-0.25	0.25-0.30	0.30-0.35	0.35-0.40	0.40-0.45	0.45-0.50	> 0.50	Total
Number of calibrators (n)	11	14	11	12	12	13	11	11	95
Number of QCs (n)	6	5	5	5	5	5	5	6	42

108

109 Table S-2. Number of samples (%) for which the predicted Hct values were within ± 0.050 L/L of the
 110 reference value (Sysmex) when applying a fivefold scan at the center of the spot or a 5-position grid
 111 (fivefold scan at different positions within the spot). For the QCs, the results obtained at Day 0 were

	Back-calculated calibrators (n = 95; RT) (%)	Back-calculated calibrators (n = 95; 60 °C) (%)	QC set 1 replicate 1 (n = 42) (%)	QC set 1 replicate 2 (n = 42) (%)	QC set 2 replicate 1 (n = 42) (%)	QC set 2 replicate 2 (n = 42) (%)
5 x center	82	82	88	90	79	79
5-position grid	88	87	90	90	93	88

112 used.

113

114 Table S-3. Accuracy (bias, % and L/L) and precision (CV, %) based on the analysis of a second set of QC
 115 samples (n = 42, n = 5 per level, except for Hct levels < 0.20 and > 0.50 L/L, where n = 6 per level).
 116 Samples were measured twice per day on 4 different days.

Hct range	Intra-day precision	Total precision	Bias	
	CV (%)	CV (%)	%	L/L
< 0.20	0.8%	1.5%	6.8%	0.012
0.20-0.25	1.4%	1.5%	2.0%	0.005
0.25-0.30	1.3%	1.3%	1.4%	0.003
0.30-0.35	1.7%	1.7%	-1.6%	-0.004
0.35-0.40	3.6%	3.6%	2.4%	0.009
0.40-0.45	2.1%	2.1%	4.1%	0.017
0.45-0.50	1.2%	1.3%	1.8%	0.009
> 0.50	1.7%	2.6%	-7.0%	-0.036
Total (42)	1.9%	1.9%	1.2%	0.002

117

118 Table S-4. Accuracy (bias, % and L/L) and precision (CV, %) based on the analysis of a first set of QC
 119 samples using the aged calibration curve (n = 42, n = 5 per level, except for Hct-levels < 0.20 and > 0.50
 120 L/L, where n = 6 per level). Samples were measured twice per day on 4 different days.

Hct range	Intra-day precision	Total precision	Bias	
	CV (%)	CV (%)	%	L/L
< 0.20	1.2%	1.8%	2.9%	0.005
0.20-0.25	1.7%	2.0%	1.4%	0.003
0.25-0.30	1.6%	2.0%	-5.2%	-0.015
0.30-0.35	1.5%	2.0%	-5.0%	-0.015
0.35-0.40	1.5%	1.7%	-5.6%	-0.019
0.40-0.45	1.4%	1.9%	-4.6%	-0.020
0.45-0.50	1.1%	1.9%	0.4%	0.002
> 0.50	2.2%	2.6%	-5.4%	-0.028
Total (42)	1.6%	2.0%	-2.6%	-0.011

121

122 Table S-5. Accuracy (bias, % and L/L) and precision (CV, %) based on the analysis of a second set of QC
 123 samples using the aged calibration curve (n = 42, n = 5 per level, except for Hct-levels < 0.20 and > 0.50
 124 L/L, where n = 6 per level). Samples were measured twice per day and on 4 different days.

Hct range	Intra-day precision	Total precision	Bias	
	CV (%)	CV (%)	%	L/L
< 0.20	0.9%	1.6%	-1.0%	-0.002
0.20-0.25	1.5%	1.6%	-4.4%	-0.010
0.25-0.30	1.3%	1.3%	-4.2%	-0.012
0.30-0.35	2.0%	2.0%	-6.5%	-0.020
0.35-0.40	1.6%	1.8%	-2.9%	-0.011
0.40-0.45	2.1%	2.1%	-0.7%	-0.003
0.45-0.50	1.2%	1.2%	-3.0%	-0.014
> 0.50	1.6%	2.5%	-11.3%	-0.058
Total (42)	1.6%	1.8%	-4.4%	-0.016

125

126

127 Table S-6. Combination of probe-to-card distance (mm) and integration time (μs) where no

Probe-to-card distance (mm)	Integration time (μs)
3	1500
4	2000
5	3000
6	4500
6.4	4500
7	4500
8	4500
9	4500
10	4500
11	4500
12	4500

128 oversaturation of the detector was observed.

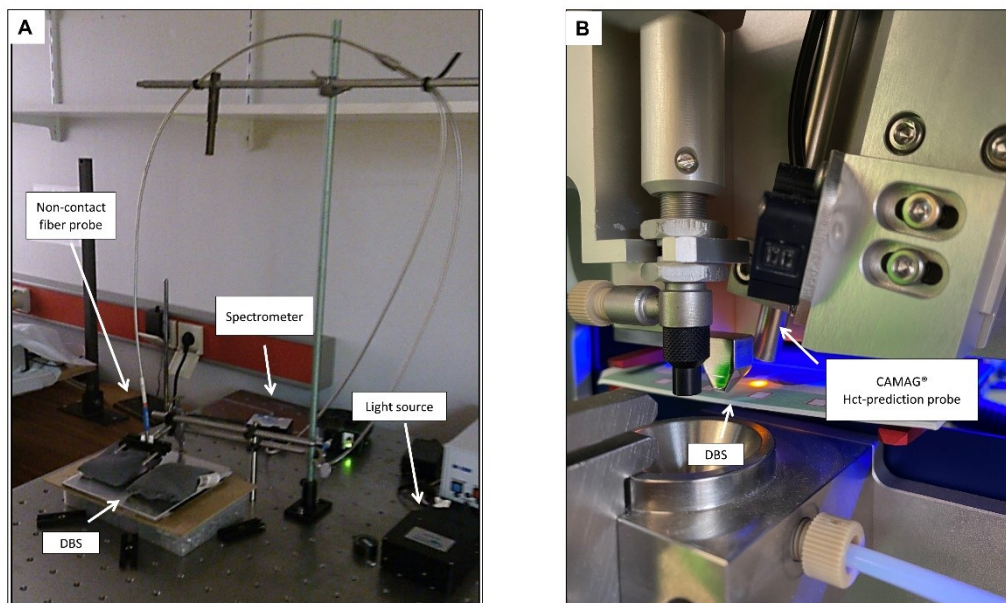
129

130 Table S-7. Number of samples ($n = 24$, %) using a certain probe-to-card distance (mm) and integration
131 time (μs) for which the difference between the back-calculated Hct and the reference (Sysmex) was
132 within ± 0.050 L/L. Back-calculated Hct levels were based on an initial, linear calibration model.

Probe-to-card distance (mm)	Integration time (μs)	Back-calculated Hct within ± 0.050 L/L of the reference (%)
3	1500	67
4	2000	75
5	3000	62
6	4500	87
6.4	4500	92
7	4500	87

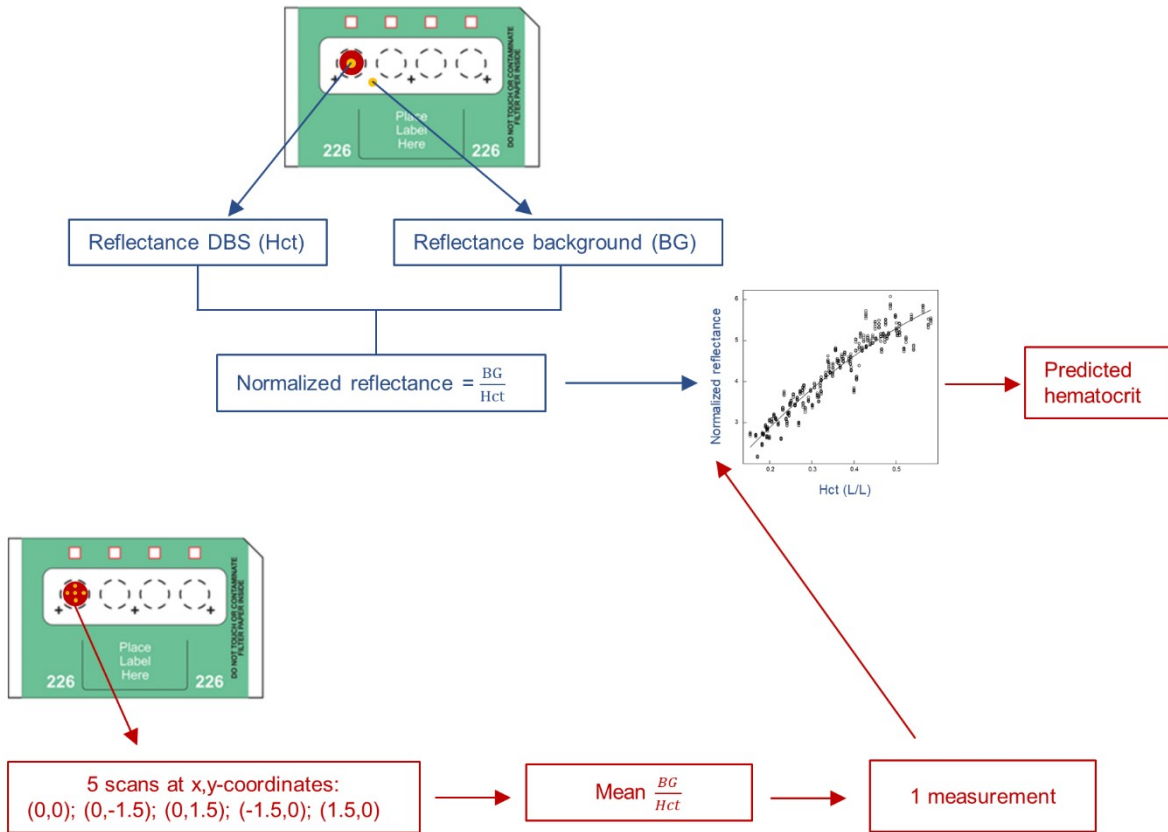
133

134 5. Supplementary Figures



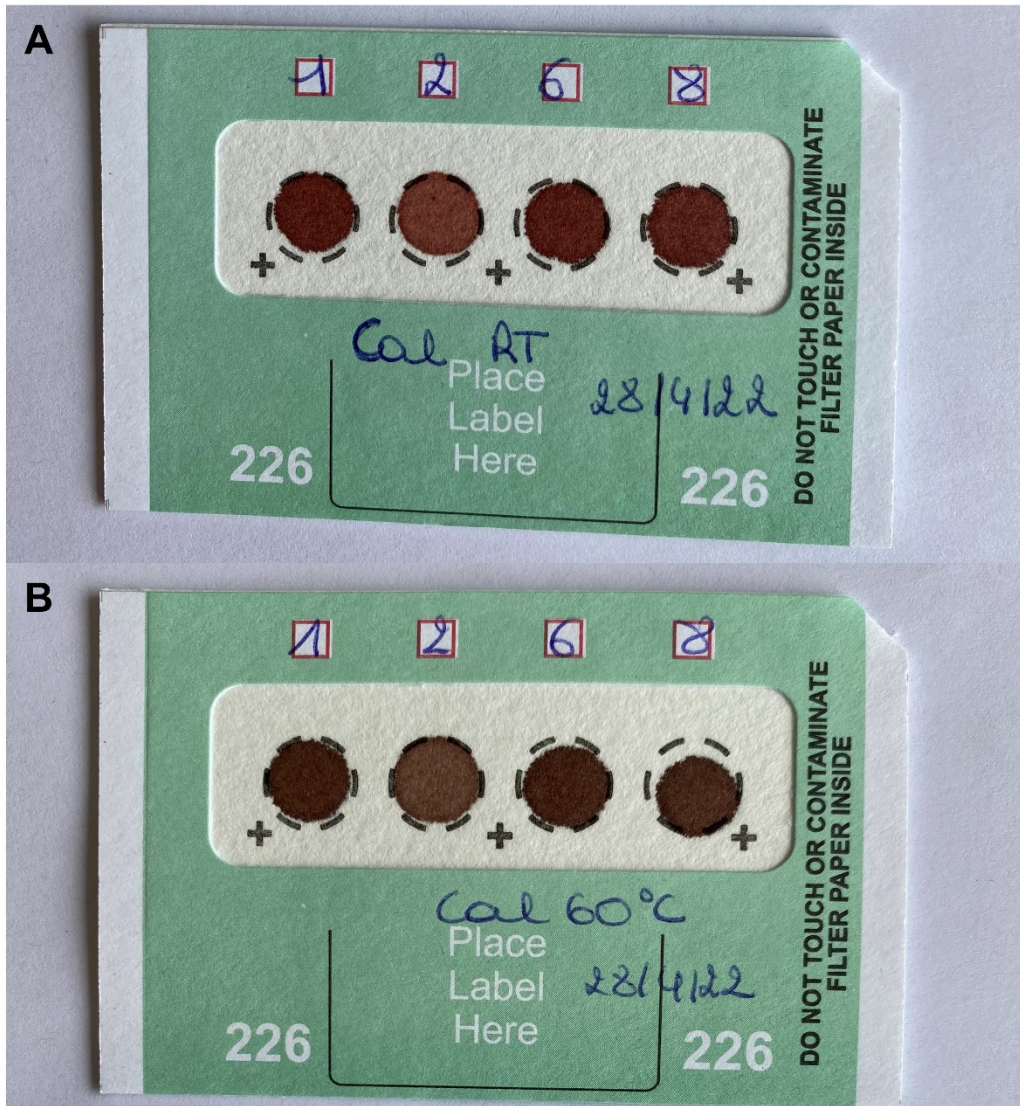
135
136 Fig. S-1. Depicted are a picture of (A) the initial, manual set-up to predict the Hct via UV-Vis
137 spectroscopy developed and described by Capiou *et al.*² and (B) the automated Hct prediction module
138 installed into the CAMAG DBS-MS 500 HCT system. The different parts required for the analysis are
139 indicated.

140



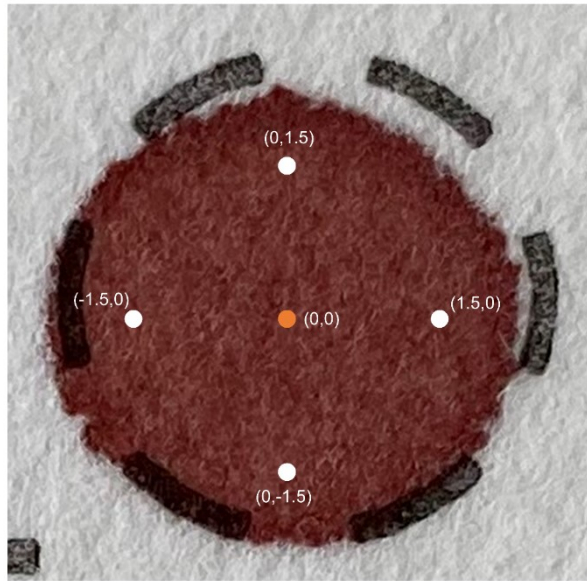
141

142 Fig. S-2. Schematic overview of how the spectral data is processed to obtain a Hct value.



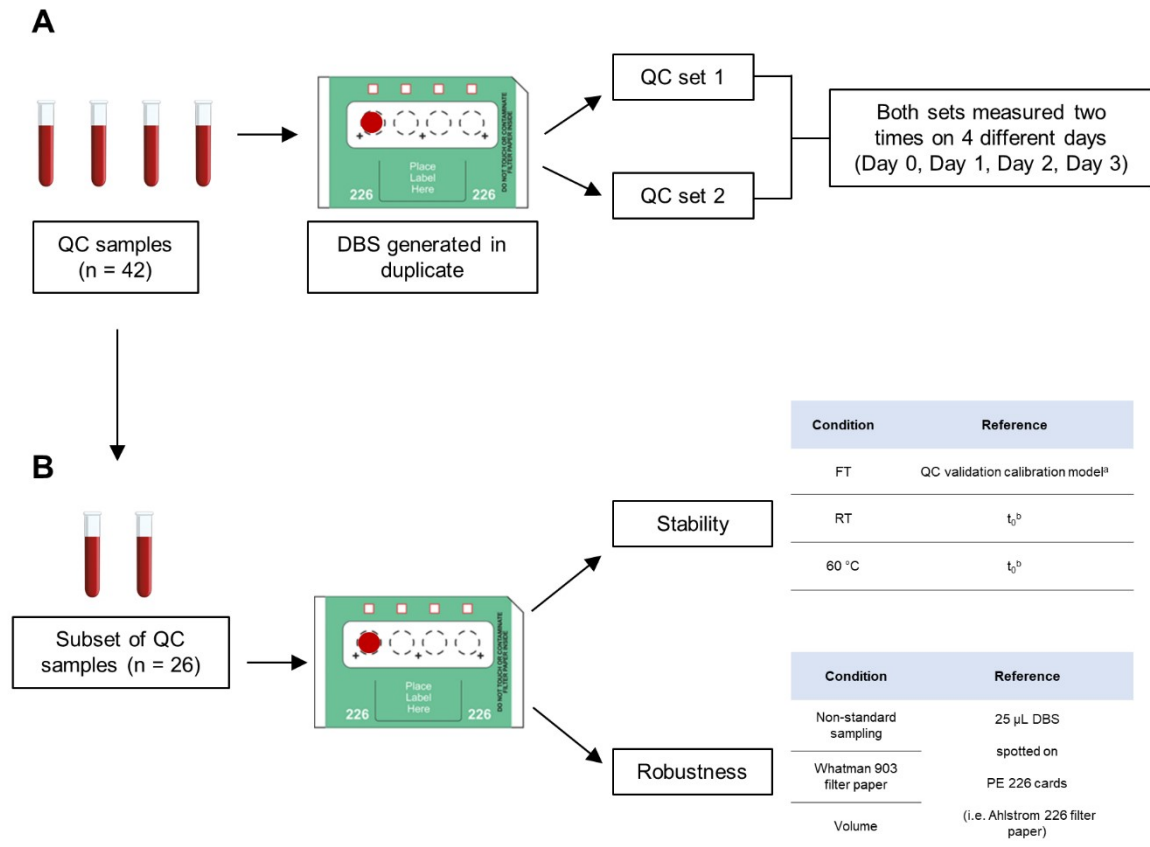
143

144 Fig. S-3. Depicted is a picture of four DBS calibration samples which were stored for 24 h (A) at room
145 temperature (RT) and (B) at 60 °C, the latter to mimic ageing of the DBS. Note the difference in color –
146 the samples stored at 60 °C being more brown.



147

148 Fig. S-4. Depicted is a 25 μ L DBS with the 5-position grid indicated by its x,y-coordinates (mm). Both
149 calibrators and QCs were scanned in fivefold at the center of the spot (orange dot) and at five different
150 positions (orange and white dots).

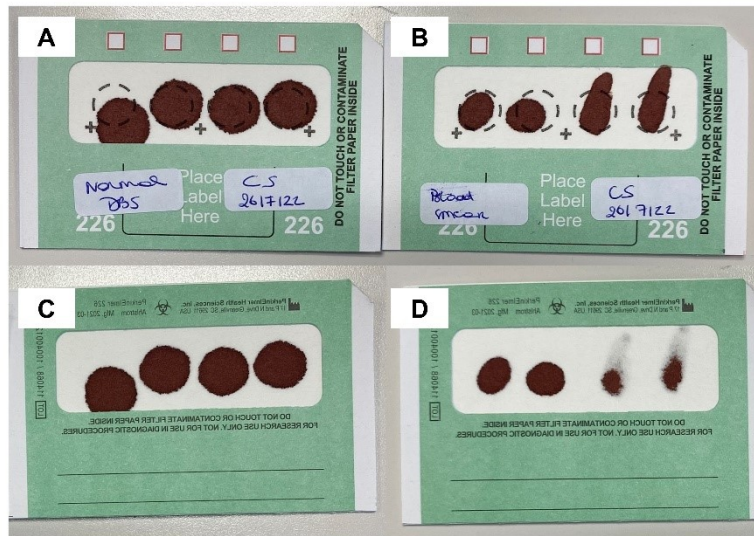


151

152 Fig. S-5. Schematic overview of (A) the analysis of the QC samples and (B) the analysis of the samples
 153 (i.e. subset of the QC samples) used for evaluation of stability and robustness and how the data analysis
 154 was performed.

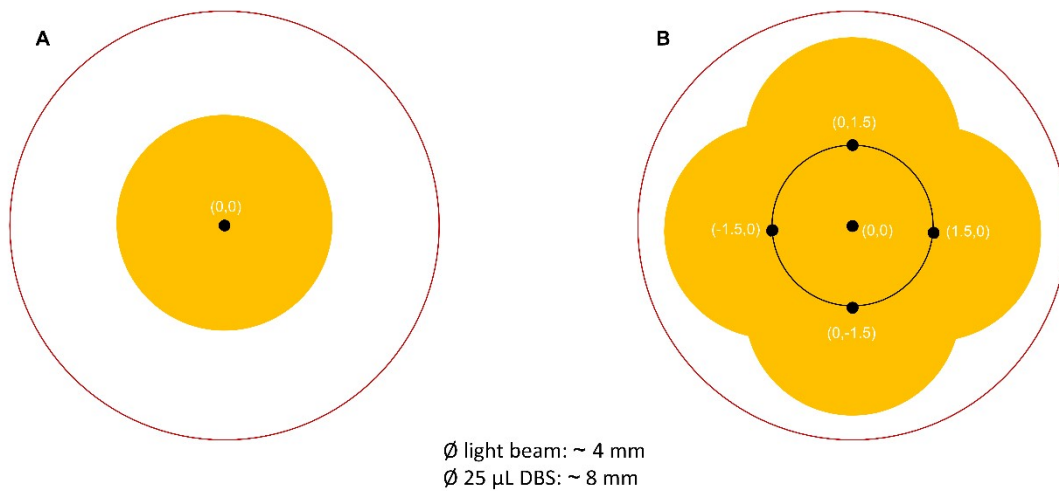
155 ^aSamples were compared to a different DBS (inter-spot comparison).

156 ^bSamples were compared to the very same DBS (intra-spot comparison).



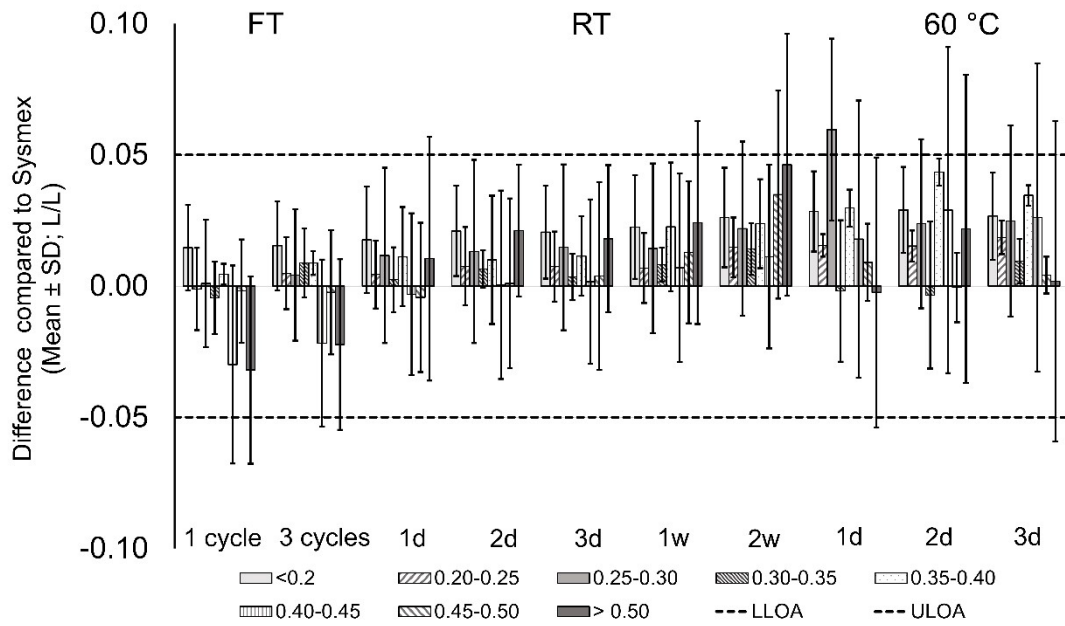
157

158 Fig. S-6. Depicted is a photograph of the front and back (the latter mirrored) of capillary DBS with a
 159 round, normal shape (A & C, respectively) and an atypical shape ('blood smear') (in B & D (3rd and 4th
 160 DBS), respectively).



161

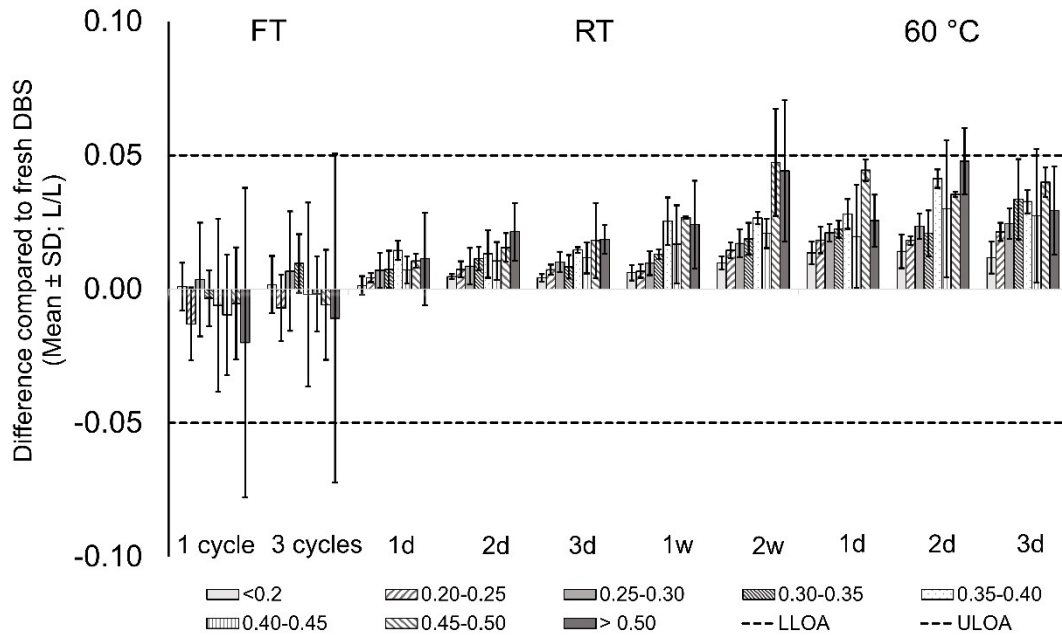
162 Fig. S-7. Approximate area of the DBS measured by the spectrophotometer (A) when no grid is used
 163 and (B) when a grid is used. The x,y-coordinates (mm) from the center are indicated in the Figures. The
 164 diameter (\varnothing) of the light beam is approximately 4 mm and the diameter of a 25 μ L DBS (used as
 165 reference) is approximately 8 mm.



166

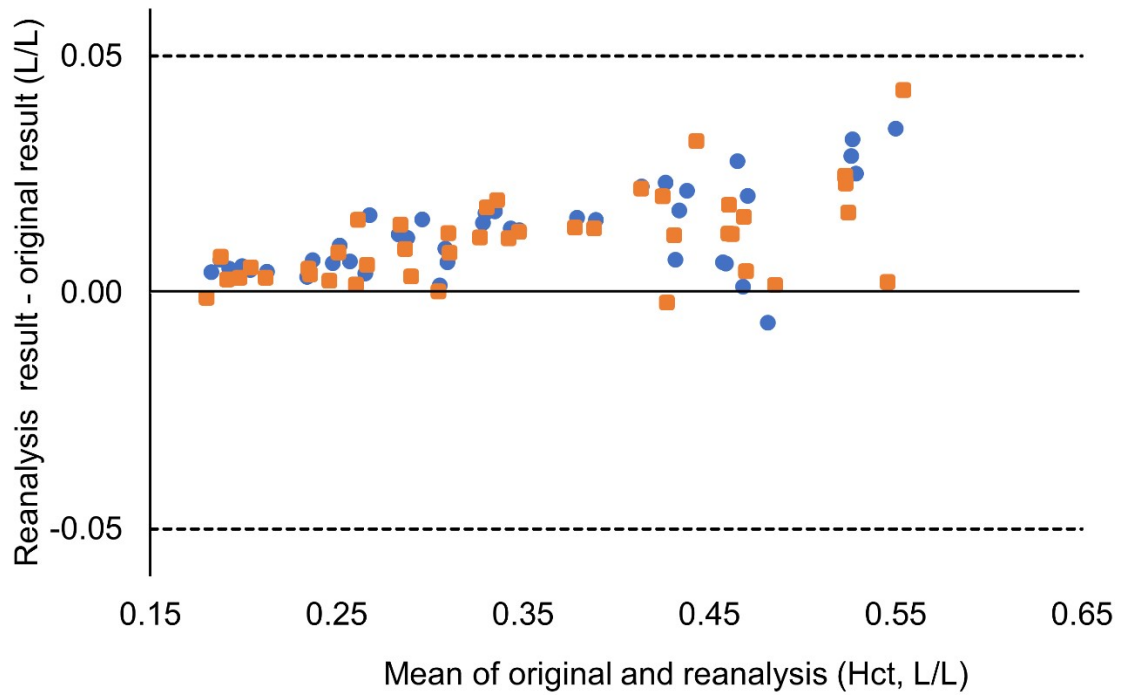
167 Fig. S-8. Stability results after one and three freeze-thaw (FT) cycles, storage at room temperature (RT)
 168 and storage at 60 °C. The mean difference \pm standard deviation (SD) per Hct level (L/L) compared to
 169 the reference value (Sysmex) is shown (n = 3 per level, except for Hct levels < 0.20 and > 0.50 L/L,
 170 where n = 4 per level). The dashed line indicates the acceptance limit of ± 0.050 L/L difference.

171



172

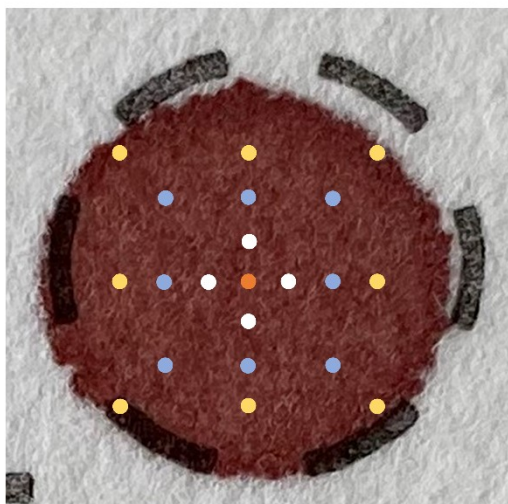
173 Fig. S-9. Stability results after one and three freeze-thaw (FT) cycles, storage at room temperature (RT)
 174 and storage at 60 °C. Results were obtained using the aged calibration curve (i.e. stored for one day at
 175 60 °C). The mean difference in Hct prediction \pm standard deviation (SD) per Hct-level (L/L) compared
 176 to fresh DBS is shown (n = 3 per level, except for Hct-levels < 0.20 and > 0.50 L/L, where n = 4 per level).
 177 The dashed line indicates the acceptance limits of ± 0.050 L/L difference.



178

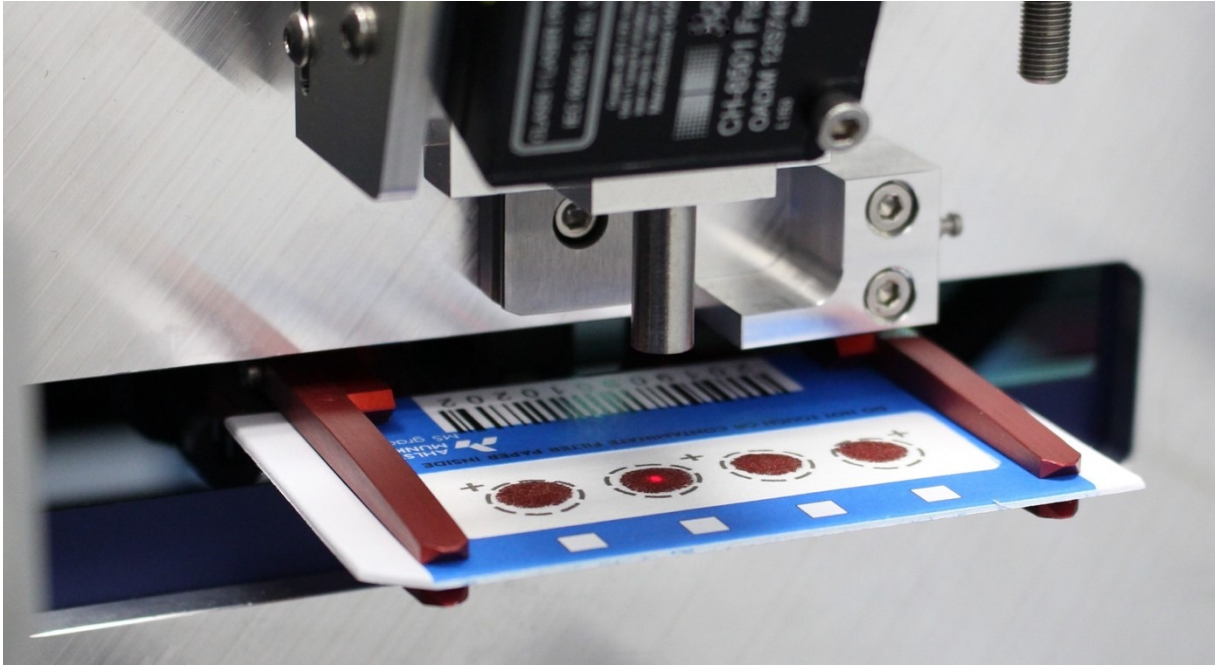
179 Fig. S-10. Incurred sample reanalysis (n = 42x2). The Hct predictions on Day 0 (DBS 1) were compared
 180 to (i) the results of the same spot (DBS 1) on Day 3 (blue circles) and (ii) the results of the replicate spot
 181 (DBS 2) on Day 3 (orange squares). The dashed line indicates the acceptance limits of ± 0.050 L/L
 182 difference, which was met by all samples.

183



184

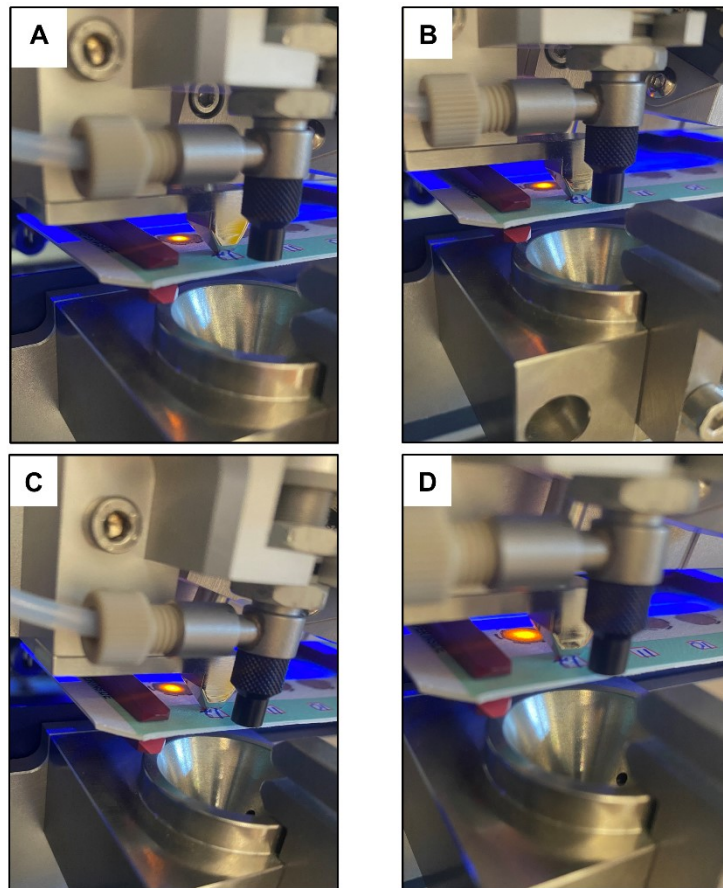
185 Fig. S-11. Depicted is a DBS where the 21 different positions where the sample was 'scanned' to
186 evaluate the ideal number of 'scans' per DBS are indicated. The center of the spot (0,0) is indicated by
187 the orange dot. The x,y-coordinates were set at 0.5 mm (white dots), 1.0 mm (blue dots) and 1.5 mm
188 (yellow dots).



189

190 Fig. S-12. Depicted is a picture of the prototype Hct prediction module (vertical probe).

191



192

193 Fig. S-13. Depicted are pictures of the automated Hct-prediction module, analyzing a DBS using
194 different probe-to-card distances: (A) 6.4 mm; (B) 7 mm; (C) 8 mm and (D) 12 mm.